

# Dynamics of Passive-Scalar Turbulence

Dhrubaditya Mitra and Rahul Pandit\*

Centre for Condensed Matter Theory, Department of Physics,  
Indian Institute of Science, Bangalore 560012, India

We present the first study of the dynamic scaling or multiscaling of passive-scalar turbulence. For the Kraichnan version of passive-scalar turbulence we show analytically, in both Eulerian and quasi-Lagrangian frameworks, that simple dynamic scaling is obtained but with different dynamic exponents. By developing the multifractal model we show that dynamic multiscaling occurs in passive-scalar turbulence only if the advecting velocity field is itself multifractal. We substantiate our results by detailed numerical simulations in shell models of passive-scalar advection.

PACS numbers: 47.27.i, 47.53.+n

Important advances have been made over the past decade in understanding the statistical properties of the turbulence of passive scalars, e.g., pollutants, and passive vectors, e.g., weak magnetic fields, advected by a fluid [1]. If the advecting velocity is stochastic and of the Kraichnan type [2], then, in some limits, it can be established analytically that passive-scalar and passive-vector turbulence show *anomalous scaling* or *multiscaling* of structure functions. These are the only turbulence problems for which such multiscaling can be proven analytically, so it is important to use them as testing grounds for new ideas about multiscaling in turbulence. We examine the dynamic-scaling properties of passive-scalar turbulence in the light of the recent systematization of dynamic multiscaling in fluid turbulence [3].

Our principal results, obtained analytically and numerically, illustrate important principles that appear, at first sight, to be surprising. We find, e.g., that the dynamic exponents depend via bridge relations only on the equal-time scaling exponents of the *velocity* field. Thus, even though equal-time structure functions for the passive-scalar problem display multiscaling, we show analytically that they exhibit *simple dynamic scaling* if the advecting velocity is of the Kraichnan type. Our study of the Kraichnan model yields the only analytical results obtained so far for time-dependent structure functions in any type of turbulence. Dynamic multiscaling is obtained only if the advecting velocity field is itself intermittent as we demonstrate numerically.

The quest for a statistical characterization of turbulence begins most often with the equal-time, order- $p$ , velocity- $u$  structure functions  $S_p^u(\ell)$ , i.e., the order- $p$  moments of the probability distribution functions (PDFs) of velocity differences at the length scale  $\ell$ . The equal-time exponents  $\zeta_p^u$  are defined by  $S_p^u(\ell) \sim \ell^{\zeta_p^u}$ , valid for the inertial range  $\eta_d \ll \ell \ll L$ , where  $\eta_d$  is the dissipation scale and  $L$  the length at which energy is pumped in. Kolmogorov's simple scaling [4](K41) yields  $\zeta_p^{u,K41} = p/3$ , but subsequent work [5] suggests significant corrections for  $p > 3$  and *multiscaling* with  $\zeta_p^u$  a nonlinear, convex, monotonically increasing function of  $p$ . The generalization of such multiscaling to *dynamic*

*multiscaling* is subtle and has been elucidated only recently [3, 6, 7, 8]: It is expected that Eulerian-velocity time-dependent structure functions [9] lead to trivial dynamic scaling with all Eulerian ( $\mathcal{E}$ ) dynamic exponents  $z_p^{u,\mathcal{E}} = 1$ . Nontrivial dynamic exponents  $z_p^u$  can be obtained [3] from dynamic-multiscaling ansätze of the form  $\tau_p^u \sim \ell^{z_p^u}$ , where the times  $\tau_p^u$  are extracted from *Lagrangian* or *quasi-Lagrangian* time-dependent structure functions. A generalization of the multifractal formalism [5] to the case of time-dependent structure functions [3, 6, 8] shows that dynamic and equal-time multiscaling exponents must be related by *bridge relations*; and these bridge relations depend crucially [3] on how time scales are extracted: In particular, time scales extracted via time derivatives of time-dependent structure functions are different from those obtained from integrals.

The advection-diffusion equation for the passive scalar field  $\theta(\mathbf{x}, t)$  at point  $\mathbf{x}$  and time  $t$  is

$$\partial_t \theta + u_i \partial_i \theta = \kappa \partial_{ii} \theta + f_\theta, \quad (1)$$

where  $\kappa$  is the passive-scalar diffusivity and  $f_\theta$  an external force. The advecting velocity  $\mathbf{u}$  should be obtained from solutions of the Navier-Stokes equation, but, to investigate equal-time multiscaling of passive-scalar structure functions, it has proved fruitful to use the *Kraichnan ensemble* in which each component of  $\mathbf{u}$  is a zero-mean, delta-correlated Gaussian random variable with

$$\langle u_i(\mathbf{x}, t) u_j(\mathbf{x} + \mathbf{r}, t') \rangle = 2D_{ij}(\mathbf{r}) \delta(t - t'). \quad (2)$$

The Fourier transform of  $D_{ij}$  has the form

$$\tilde{D}_{ij}(\mathbf{q}) \propto \left( q^2 + \frac{1}{L^2} \right)^{-\frac{d+\xi}{2}} e^{-\eta q^2} \left[ \delta_{ij} - \frac{q_i q_j}{q^2} \right], \quad (3)$$

where  $\mathbf{q}$  is the wave-vector,  $d$  the spatial dimension,  $\eta$  the dissipation scale,  $L$  the large forcing scale, and  $\xi$  a parameter. The term inside square brackets assures incompressibility. In real space, if we write  $D_{ij}(\mathbf{r}) \equiv D^0 \delta_{ij} - \frac{1}{2} d_{ij}(\mathbf{r})$  and take the limits  $L \rightarrow \infty$  and  $\eta \rightarrow 0$ , we get

$$d_{ij} = D_1 r^\xi \left[ (d-1+\xi) \delta_{ij} - \xi \frac{r_i r_j}{r^2} \right], \quad (4)$$

with  $D_1$  a normalization constant. For  $0 < \xi < 2$  this model shows multiscaling of equal-time, order- $p$ , passive-scalar structure functions [1]. The constant  $D^0 \equiv 2 \int_0^\infty \tilde{D}_{ij}(\mathbf{q}) d^d q \propto O(L^\xi)$  diverges in the limit  $L \rightarrow \infty$ . The external force  $f_\theta$  is also a zero-mean, Gaussian random variable which is white-in-time with the variance  $\langle f_\theta(\mathbf{x}, t) f_\theta(\mathbf{y}, t') \rangle = C \left( \frac{|\mathbf{x} - \mathbf{y}|}{L} \right) \delta(t - t')$ , where the function  $C(x/L)$  is confined to large length scales. Moreover,  $f_\theta$  and  $\mathbf{u}$  are statistically independent.

The quasi-Lagrangian transformation of any Eulerian field  $\psi(\mathbf{x}, t)$  is defined by  $\hat{\psi}(\mathbf{x}, t) \equiv \psi[\mathbf{x} + \mathbf{R}(t; \mathbf{r}_0, 0), t]$ , where  $\mathbf{R}(t; \mathbf{r}_0, 0)$  is the Lagrangian trajectory passing through  $\mathbf{r}_0$  at  $t = 0$  [10]. Thus the quasi-Lagrangian version of Eq. (1) is

$$\partial_t \hat{\theta} + [\hat{u}_i - \hat{u}_i(0)] \partial_i \hat{\theta} = \kappa \partial_{ii} \hat{\theta} + \hat{f}_\theta. \quad (5)$$

The equal-time multiscaling properties of passive-scalar structure functions in the Kraichnan model, well understood in the Eulerian framework, remain unchanged in the quasi-Lagrangian framework [1]. We concentrate on the time-dependent structure functions

$$\mathcal{F}_p^\phi(\mathbf{r}, \{t_1, \dots, t_p\}) \equiv \langle [\delta\phi(\mathbf{x}, t_1, \mathbf{r}) \dots \delta\phi(\mathbf{x}, t_p, \mathbf{r})] \rangle, \quad (6)$$

where  $\phi$  is  $\theta$  or  $\hat{\theta}$  in the Eulerian or quasi-Lagrangian frameworks, respectively, the angular brackets denote an average over the PDFs of  $\mathbf{u}$  and  $f_\theta$ , and  $\delta\phi(\mathbf{x}, t, \mathbf{r}) \equiv \phi(\mathbf{x} + \mathbf{r}, t) - \phi(\mathbf{x}, t)$ . Dimensional analysis yields the  $r$ -dependent characteristic time  $\mathcal{T}(r) \sim \frac{r^2}{D_{ij}(r)} \sim r^{2-\xi}$ , whence  $z_p^\theta = 2 - \xi$  for all  $p$ . Like the K41 result  $z_p^u = 2/3$  for fluid turbulence, we expect this prediction to be valid for the passive-scalar case in Lagrangian or quasi-Lagrangian frameworks. For  $p = 2$ ,  $\mathcal{F}_2^\theta(r, t) = 2C^\theta(\mathbf{0}, t) - 2C^\theta(\mathbf{r}, t)$ , where  $C^\theta(\mathbf{r}, t) \equiv \langle \phi(\mathbf{x} + \mathbf{r}, t) \phi(\mathbf{x}, 0) \rangle$ . Equations for  $C^\theta(\mathbf{r}, t)$ , obtained from Eqs. (1) and (5) by Gaussian averaging [5] over the PDFs of  $\mathbf{u}$  and  $f_\theta$  [14], are (in the  $\kappa \rightarrow 0$  limit of relevance to turbulence)

$$\partial_t C^\theta(\mathbf{r}, t) = D^0(L) \partial_{ii} C^\theta \sim L^\xi \partial_{ii} C^\theta; \quad (7)$$

$$\partial_t C^{\hat{\theta}}(\mathbf{r}, t) = (D^0 \delta_{ij} - D_{ij}) \partial_{ij} C^{\hat{\theta}} \sim d_{ij}(\mathbf{r}) \partial_{ij} C^{\hat{\theta}}. \quad (8)$$

Spatial Fourier transforms of Eqs. (7) or (8) then yield  $\tilde{C}^\phi(\mathbf{q}, t) \sim \exp[-t/\tau^\phi(\mathbf{q})]$ , with characteristic time scales  $\tau^\theta = [D^0(L)q]^{-2}$  [Eq. (7)] and  $\tau^{\hat{\theta}} \sim q^{\xi-2}$  [Eq. (8)]. The last term of Eq. (7) diverges as  $L \rightarrow \infty$ , a signature of the sweeping effect; however, for a fixed integral scale  $L$ , the Fourier transform of Eq. (7) implies  $z_2^\theta = 2$  (cf.  $z_p^{u, \mathcal{E}} = 1$ ). This sweeping divergence is removed in Eq. (8), whose Fourier transform, in the limit  $L \rightarrow \infty$ , gives  $z_2^{\hat{\theta}} = 2 - \xi$ , which agrees with the dimensional prediction. These results are remarkable for two reasons: (1) this is the first calculation of dynamic scaling exponents in any form of turbulence and (2) this shows explicitly how sweeping

effects are removed in the quasi-Lagrangian representation. Similar, but more cumbersome, calculations yield  $z_4^\theta = 2$  and  $z_4^{\hat{\theta}} = 2 - \xi$ , which we substantiate by our numerical studies below [15].

A turbulent velocity field obeying the Navier-Stokes equation does not have simple statistical properties as in Eq. (2), so we use the multifractal model [5] and its extension to dynamic multiscaling [3]. To eliminate the sweeping effect, we consider the structure functions, namely  $\mathcal{F}_p^{\hat{\theta}}(r, t)$ , namely,

$$\frac{\mathcal{F}_p^{\hat{\theta}}(r, t)}{(\hat{\theta}_L)^p} \propto \int_{\mathcal{I}} d\mu(h) \left( \frac{r}{L} \right)^{3+ph-D(h)} \mathcal{G}^{p,h} \left( \frac{t}{\tau_{p,h}} \right), \quad (9)$$

where  $\hat{\theta}$  is assumed to possess a range of universal scaling exponents  $h \in \mathcal{I} \equiv (h_{min}, h_{max})$ . For each  $h$  in this range, there exists a set  $\Sigma_h \subset \mathbb{R}^3$  of fractal dimension  $D(h)$ , such that  $\frac{\delta\hat{\theta}(\mathbf{x}, r)}{\hat{\theta}_L} \propto \left( \frac{r}{L} \right)^h$  for  $\mathbf{x} \in \Sigma_h$ , with  $\hat{\theta}_L$  the passive-scalar variable at the forcing scale  $L$ .  $\mathcal{G}^{p,h} \left( \frac{t}{\tau_{p,h}} \right)$  has a characteristic decay time  $\tau_{p,h} \sim r/\delta u(r)$  [16],  $\mathcal{G}^{p,h}(0) = 1$ , and the velocity field is also multifractal with a range of universal scaling exponents  $g \in \mathcal{I} \equiv (g_{min}, g_{max})$ . Following Ref. [3] we define the order- $p$ , degree- $M$ , *integral* time scale  $\mathcal{T}_{p,M}^{\hat{\theta}, I}(r) \equiv \left[ \frac{1}{S_p^{\hat{\theta}}(r)} \int_0^\infty \mathcal{F}_p^{\hat{\theta}}(r, t) t^{(M-1)} dt \right]^{(1/M)}$  and the *derivative* time scale  $\mathcal{T}_{p,M}^{\hat{\theta}, D} \equiv \left[ \frac{1}{S_p^{\hat{\theta}}(r)} \frac{\partial^M}{\partial t^M} \mathcal{F}_p^{\hat{\theta}}(r, t) \Big|_{t=0} \right]^{(-1/M)}$ , with corresponding dynamic-multiscaling exponents defined via  $\mathcal{T}_{p,M}^{\hat{\theta}, I} \sim r^{z_{p,M}^{\hat{\theta}, I}}$  and  $\mathcal{T}_{p,M}^{\hat{\theta}, D} \sim r^{z_{p,M}^{\hat{\theta}, D}}$ . To calculate

$$\mathcal{T}_{p,1}^{\hat{\theta}, I}(r) \propto \frac{1}{S_p^{\hat{\theta}}(r)} \int_{\mathcal{I}} d\mu(h) \left( \frac{r}{L} \right)^{3+ph-D(h)} \int_0^\infty \mathcal{G}^{p,h} \left( \frac{t}{\tau_{p,h}} \right) dt, \quad (10)$$

e.g., we substitute the multifractal form (9), do the time integral first, and use the scaling ansatz for  $\tau_{p,h}$  and we obtain  $\mathcal{T}_{p,1}^{\hat{\theta}, I}(r) \propto r^{1-\zeta_p^{\hat{\theta}, I}} \langle (\delta\theta)^p (\delta u)^{-1} \rangle$ . Following Ref. [12][17], if we now assume that the dominant contribution to

$$\langle (\delta\theta)^p (\delta u)^{-q} \rangle \approx \langle (\delta\theta)^p \rangle \langle (\delta u)^{-q} \rangle, \quad (11)$$

we have  $z_{p,M}^{\hat{\theta}, I} = 1 - |\zeta_{-1}^u|$ . Similar calculations yield the following more general bridge-relations

$$z_{p,M}^{\hat{\theta}, D} = 1 - \frac{\zeta_M^u}{M}, \quad z_{p,M}^{\hat{\theta}, I} = 1 - \frac{|\zeta_{-M}^u|}{M}, \quad (12)$$

which do not depend on  $p$ . However, this does not mean we have simple dynamic scaling. For a velocity field which multiscales, i.e., for which  $\zeta_M^u/M \neq \zeta_1^u$ , we have dynamic multiscaling. For the Kraichnan model a similar multifractal formalism predicts  $z_{p,1}^{\hat{\theta}, D} = 2 - \xi$ .

We now substantiate our analytical and multifractal results by detailed numerical simulations of shell-model analogs of the two passive-scalar problems discussed above. For this purpose we consider two very similar shell models, A and B, of the general form [11, 12]

$$\left[\frac{d}{dt} + \kappa k_m^2\right]\hat{\theta}_m(t) = i\Phi_{m,\hat{\theta}\hat{u}}^{A/B} + \delta_{m,1}f(t). \quad (13)$$

For model A, which corresponds to the Kraichnan model,  $\Phi_{m,\hat{\theta}\hat{u}}^A = [(k_m/2)(\hat{\theta}_{m+1}^*\hat{u}_{m-1}^* - \hat{\theta}_{m-1}^*\hat{u}_{m+1}^*) + (-k_{m-1}/2)(\hat{\theta}_{m-1}^*\hat{u}_{m-2}^* + \hat{\theta}_{m-2}^*\hat{u}_{m-1}^*) + (k_{m+1}/2)(\hat{\theta}_{m+2}^*\hat{u}_{m+1}^* + \hat{\theta}_{m+1}^*\hat{u}_{m+2}^*)]$ . Here the asterisk denotes complex conjugation,  $\theta_m$  and  $\hat{u}_m$  are, respectively, shell-model analogs of the Fourier components of the passive scalar and velocity in the quasi-Lagrangian framework,  $k_m = 2^m k_0$  and  $k_0 = 1/16$ . The shell velocity is a zero-mean, Gaussian random complex variable with covariance  $\langle \hat{u}_m(t)\hat{u}_n^*(t') \rangle = D_m \delta_{m,n} \delta(t-t')$ ,  $D_m = k_m^{-\xi}$ ,  $f(t)$  is random, Gaussian and white-in-time and independent of  $\hat{u}_m$ . In model B,  $\Phi_{m,\hat{\theta}\hat{u}}^B = [k_m(\hat{\theta}_{m+1}\hat{u}_{m-1} - \hat{\theta}_{m-1}\hat{u}_{m+1}) - (k_{m-1}/2)(\hat{\theta}_{m-1}\hat{u}_{m-2} + \hat{\theta}_{m-2}\hat{u}_{m-1}) - (k_{m+1}/2)(\hat{\theta}_{m+2}\hat{u}_{m+1} + \hat{\theta}_{m+1}\hat{u}_{m+2})]^*$ . This is the shell-model analog of a passive scalar advected by a Navier-Stokes velocity field. Here the shell velocity obeys the GOY shell-model equation [5, 13]

$$\left[\frac{d}{dt} + \nu k_m^2\right]\hat{u}_m = i\Gamma_{m,\hat{u}\hat{u}} + \delta_{m,1}f^{\hat{u}}, \quad (14)$$

where  $\Gamma_{m,\hat{u}\hat{u}} = [k_m\hat{u}_{m+1}\hat{u}_{m+2} - \delta k_{m-1}\hat{u}_{m-1}\hat{u}_{m+1} - (1-\delta)k_{m-2}\hat{u}_{m-1}\hat{u}_{m-2}]^*$  with  $\delta = 1/2$ . For both models A and B,  $\hat{u}_{-1} = \hat{u}_0 = \hat{\theta}_{-1} = \hat{\theta}_0 = 0$ , and the couplings are limited to next-nearest-neighbor shells, hence the dynamic scaling or multiscaling properties of time-dependent structure functions should be akin to those of quasi-Lagrangian variables [3] (so we use  $\hat{\theta}_m$  and  $\hat{u}_m$ ). Furthermore, when  $\nu \rightarrow 0$  and  $f^{\hat{u}} \rightarrow 0$ ,  $E^{\hat{\theta}} \equiv \sum_{m=1}^N |\hat{\theta}_m|^2$  is conserved, where  $N$  is the total number of shells. We use a weak, order-one, Euler scheme associated with the Ito formulation of Eq. (13) to integrate model A and a second-order Adams-Bashforth scheme to integrate model B. The different parameters used in our simulations, e.g., the large-eddy-turnover-time  $\tau_L$ , are given in Table (I). The shell-model equal-time passive-scalar structure functions are  $S_p(m) \equiv \langle [\hat{\theta}_m \hat{\theta}_m^*]^{p/2} \rangle \sim k_m^{-\zeta_p^{\hat{\theta}}}$ . Model A exhibits equal-time multiscaling for  $0 < \xi < 2$ ; we use  $\xi = 0.6$  here. The equal-time multiscaling exponents for model B are given in the second column of Table II. Our results for the equal-time multiscaling exponents  $\zeta_p^{\hat{\theta}}$  for both models A and B agree well with previous studies (Ref. [11] for model A and Ref. [12] for model B). We now define the order- $p$ , time-dependent,

Model	$\kappa$	$\delta t$	$\tau_L$	$T_{tr}$	$T_{av}$
A	$2^{-14}$	$2^{-24}$	$\simeq 2^{24}\delta t$	$5 \times 10^4 \tau_L$	$10^5 \tau_L$
B	$5 \times 10^{-7}$	$10^{-4}$	$10^5 \delta t$	$5 \times 10^4 \tau_L$	$10^5 \tau_L$

TABLE I: The diffusivity  $\kappa$ , the time-step  $\delta t$ , and the box-size eddy turnover time  $\tau_L \equiv 1/k_0 u_{rms}$  that we use in our simulations of models A and B. Data from the first  $T_{tr}$  time steps are discarded so that transients can die down. We then average our data for time-dependent structure functions for an averaging time  $T_{av}$ . For model A we use  $\xi = 0.6$ . The number of shells  $N = 22$  for both the models.

order( $p$ )	$\zeta_p^{\hat{\theta}}$	$z_{p,1}^{\hat{\theta},I}$	$z_{p,2}^{\hat{\theta},D}$
1	$0.34 \pm 0.001$	$0.52 \pm 0.03$	$0.63 \pm 0.03$
2	$0.63 \pm 0.001$	$0.53 \pm 0.03$	$0.64 \pm 0.03$
3	$0.87 \pm 0.001$	$0.56 \pm 0.005$	$0.64 \pm 0.005$
4	$1.07 \pm 0.001$	$0.56 \pm 0.005$	$0.64 \pm 0.01$
5	$1.24 \pm 0.004$	$0.56 \pm 0.005$	$0.64 \pm 0.01$
6	$1.38 \pm 0.006$	$0.57 \pm 0.007$	$0.64 \pm 0.02$

TABLE II: Order- $p$  (Column 1) multiscaling exponents for  $1 \leq p \leq 6$  from our simulations of model B: equal-time exponents  $\zeta_p^{\hat{\theta}}$  (Column 2), integral-scale dynamic-multiscaling exponent  $z_{p,1}^{\hat{\theta},I}$  of degree-1 (Column 3) and derivative-time dynamic-multiscaling exponents  $z_{p,2}^{\hat{\theta},D}$  (Column 4) from our calculations. We obtain (1)  $z_{p,1}^{\hat{\theta},I} = 0.56 \pm 0.005$  from the bridge-relation (12) and  $\zeta_{-1}^u = -0.44 \pm 0.005$ ; (2)  $z_{p,2}^{\hat{\theta},D} = 0.645 \pm 0.0001$  from the bridge relation and  $\zeta_2^u = 0.709 \pm 0.0001$ . See text for error estimates.

passive-scalar structure functions for our shell models:

$$F_p(m, t) \equiv \frac{1}{S_p(m)} \langle [\hat{\theta}_m(0)\hat{\theta}_m^*(t)]^{p/2} \rangle. \quad (15)$$

For model A an analytical calculation yields [cf. Eq. (7)]

$$F_2(m, t) = S_2(m) \exp\left[-\frac{1}{4}k_m^{2-\xi}A(\xi)t\right], \quad (16)$$

where  $A(\xi) = [2^{(2\xi-2)} + 2^{-(2\xi-2)}] + (2^\xi + 2^{-\xi}) + (2^{(\xi-2)} + 2^{-(\xi-2)})$ , whence  $z_2^{\hat{\theta}} = 2 - \xi$ . Similar relations can be derived for  $p \geq 4$  but the complexity increases with  $p$ .

For model A we fit an exponential to each of  $F_p(m, t)$  up to a time  $t_\mu$ , such that  $\frac{F_p(m, t_\mu)}{S_p(m)} = \mu$ , to extract a characteristic decay rate  $T_p(m)$ . We use  $\mu = 0.7$ ; we find that values of  $\mu$  from 0.5 to 0.9 do not change our results significantly. Representative plots for  $p = 4$  are shown in Fig. (1 a). The slopes of these and similar plots yield  $z_2^{\hat{\theta}} = 1.400 \pm 0.005$ ,  $z_4^{\hat{\theta}} = 1.400 \pm 0.005$ ,  $z_6^{\hat{\theta}} = 1.40 \pm 0.01$ , which clearly support our analytical result  $z_p^{\hat{\theta}} = 2 - \xi$  with  $\xi = 0.6$ . For model B the imaginary parts of  $F_p(m, t)$  are negligible compared to their real parts. Henceforth we consider only the real

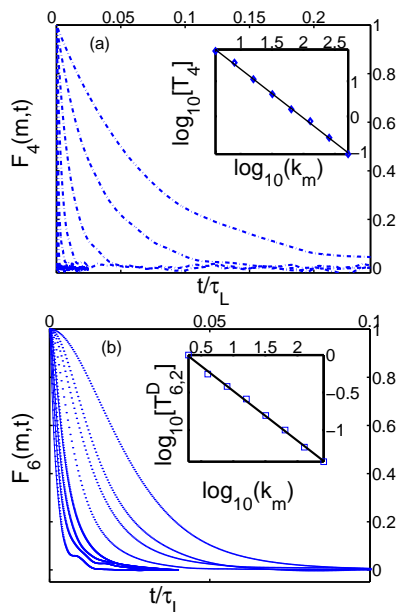


FIG. 1: (a) Plot of the order-4 time-dependent structure function for model A, with  $\xi = 0.6$ , versus  $t/\tau_L$ , for shells  $m = 6$  to 13 (the last few are not clearly visible). Exponential functions [like Eq. (16)] are good approximations for these time-dependent structure functions. The inset shows a log-log plot of  $T_4^{\hat{\theta}}$  against the wavevector  $k_m$ ; the slope of the straight line (least-squares fit) gives  $z_4^{\hat{\theta}} \simeq 1.40 \simeq 2 - \xi$ . (b) A plot as in (a) for model B, for  $p = 6$ . The inset shows a log-log plot of  $T_{6,2}^D$  versus the wavevector  $k_m$ ; the straight line is the least-squares fit to the points.

part. We use two different sampling rates,  $50 \times \delta t$  for  $4 \leq m \leq 8$  and  $10 \times \delta t$  for  $9 \leq m \leq 13$ , respectively. For extracting  $T_{p,2}^D$  we extend  $F_p(m, t)$  to negative  $t$  via  $F_p(m, -t) = F_p(m, t)$  and use a centered, sixth-order, finite-difference scheme to find  $\frac{\partial^2}{\partial t^2} F_p(m, t)|_{t=0}$ . A log-log plot of  $T_{p,2}^D$  versus  $k_m$  now yields the exponents  $z_{p,2}^{\hat{\theta},D}$  given in Table (II). A comparison of our results with the multifractal prediction of Eq.(12) is shown in Table (II). We have computed the integral time scale only for  $M = 1$ , i.e.,  $T_{p,1}^I(m, t_u) \equiv \int_0^{t_u} F_p(m, t) dt \sim k_m^{-z_{p,1}^{\hat{\theta},I}}$  [18]. In principle we should use  $t_u \rightarrow \infty$  but, since it is not possible to obtain  $F_p(m, t)$  accurately for large  $t$ , we select an upper cut-off  $t_u$  such that  $F_p(m, t_u) = \alpha$ , where, for all  $m$  and  $p$ , we choose  $\alpha = 0.7$ . We have checked that our results do not change if we use  $0.3 < \alpha < 0.8$ . The slope of a log-log plot of  $T_{p,1}^I(m)$  versus  $k_m$  now yields  $z_{p,1}^{\hat{\theta},I}$  shown in Table (II). The difference between the dynamic-scaling exponents of integral and derivative type (Columns 3 and 4 of Table (II), respectively) is a clear signature of dynamic multiscaling.

To obtain the error-bars on the equal-time and dynamic exponents, we carry out 50 runs, each averaged over a time  $T_{av}$  given in Table (I). We thus obtain 50 different values for each of these exponents. The mean val-

ues of these 50 exponents are quoted here [Table (II)]; and the root-mean-square deviation about the mean value yields the error estimates shown in Table (II). Note that the low-order dynamic structure functions decay slowly and hence, for a fixed averaging time, low-order dynamic multiscaling exponents have larger error bars than those of slightly higher-order exponents.

We have shown that, for passive-scalar turbulence, simple dynamic scaling is obtained if the velocity field is of the Kraichnan type. Dynamic multiscaling is obtained if the advecting velocity is itself multifractal. The study of dynamic multiscaling in passive-vector turbulence is more complicated because of the dynamo effect and will be dealt with elsewhere. The experimental study of such dynamic multiscaling remains an important challenge.

We thank A. Celani, S. Ramaswamy and M. Vergassola for discussions and IFCPAR (Project no. 2404-2) and CSIR (INDIA) for financial support.

\* Also at Jawaharlal Nehru Centre For Advanced Scientific Research, Jakkur, Bangalore, India

- [1] G. Falkovich, K. Gawędzki, and M. Vergassola, *Rev. Mod. Phys.* **73**, 913 (2001).
- [2] R. Kraichnan, *Phys. Fluids* **11**, 945 (1968).
- [3] D. Mitra and R.Pandit, *Phys. Rev. Lett* **93**, 024501 (2004).
- [4] A. Kolmogorov, *Dokl. Acad. Nauk USSR* **30**, 9 (1941).
- [5] U. Frisch, *Turbulence the legacy of A.N. Kolmogorov* (Cambridge University Press, Cambridge, 1996).
- [6] V. L'vov, E. Podivilov, and I. Procaccia, *Phys. Rev. E* **55**, 7030 (1997).
- [7] F. Hayot and C. Jayaprakash, *Phys. Rev. E* **57**, R4867 (1998).
- [8] D. Mitra and R.Pandit, *Physica A* **318**, 179 (2003).
- [9] Y. Kaneda, T. Ishihara, and K. Gotoh, *Phys. Fluids* **11**, 2154 (1999).
- [10] V. Belinicher and V. L'vov, *Sov. Phys. JETP* **66**, 303 (1987).
- [11] A. Wirth and L. Biferale, *Phys. Rev. E* **54**, 4928 (1996).
- [12] M. Jensen, G. Paladin, and A. Vulpiani, *Phys. Rev. A* **45**, 7214 (1992).
- [13] E. Gledzer, *Sov. Phys. Dokl.* **18**, 216 (1973); K. Ohkitani and M. Yamada, *Prog. Theor. Phys.* **55**, 833 (1985); L. Kadanoff, D. Lohse, J. Wang, and R. Benzi, *Phys. Fluids* **7**, 617 (1999).
- [14] The equation for  $C^\phi(\mathbf{r}, t)$  is closed only for strictly positive  $t$ , and this is the case we consider.
- [15] For such simple scaling the integral and derivative time scales of course yield the same dynamic-scaling exponent.
- [16] This is the simplest ansatz for  $\tau_{p,h}$  [3].
- [17] As shown in Ref. [12], this assumption is equivalent to assuming strong correlation between the flux of the velocity and the passive-scalar variable which leads to good agreement of  $\zeta_p^\theta$  with experimental data. We have checked that this assumption holds true for our shell model simulations for  $p, q = 1, \dots, 6$ .
- [18] We have checked that  $\zeta_p^u$  are well defined here only for  $p > -1.84$  so we must have  $M < 1.84$  via Eq. (12).